Development 133, 1263-1275 (2006) doi:10.1242/dev.02300

FGF negatively regulates muscle membrane extension in *Caenorhabditis elegans*

Scott J. Dixon[1], Mariam Alexander, Raynah Fernandes, Nicole Ricker and Peter J. Roy[1,*]

Striated muscles from *Drosophila* and several vertebrates extend plasma membrane to facilitate the formation of the neuromuscular junction (NMJ) during development. However, the regulation of these membrane extensions is poorly understood. In *C. elegans*, the body wall muscles (BWMs) also have plasma membrane extensions called muscle arms that are guided to the motor axons where they form the postsynaptic element of the NMJ. To investigate the regulation of muscle membrane extension, we screened 871 genes by RNAi for ectopic muscle membrane extensions (EMEs) in *C. elegans*. We discovered that an FGF pathway, including *let-756*(FGF), *egl-15*(FGF receptor), *sem-5*(GRB2) and other genes negatively regulates plasma membrane extension from muscles. Although compromised FGF pathway activity results in EMEs, hyperactivity of the pathway disrupts larval muscle arm extension, a phenotype we call muscle arm extension defective or MAD. We show that expression of *egl-15* and *sem-5* in the BWMs are each necessary and sufficient to prevent EMEs. Furthermore, we demonstrate that *let-756* expression from any one of several tissues can rescue the EMEs of *let-756* mutants, suggesting that LET-756 does not guide muscle membrane extensions. Our screen also revealed that loss-of-function in laminin and integrin components results in both MADs and EMEs, the latter of which are suppressed by hyperactive FGF signaling. Our data are consistent with a model in which integrins and laminins are needed for directed muscle arm extension to the nerve cords, while FGF signaling provides a general mechanism to regulate muscle membrane extension.

KEY WORDS: Muscle arms, Muscle development, Elegans, FGF, RNAi, Integrin

INTRODUCTION

Plasma membrane extension is central to both development and disease. Epiboly, ingression, axon extension and cell migration are all processes in animal development that require actin-based membrane extension at the leading edge of the cell (Pollard and Borisy, 2003). This activity is often hijacked in cancerous cells to promote neo-vascularization of tumors (Folkman, 1971; Ogawa et al., 2000; Plate et al., 1992) and the metastatic colonization of healthy tissue (Keilhack et al., 2001). Many of these migrations and cell extensions are regulated by well characterized guidance cues, cell-surface receptors and downstream signaling elements that function together to control cytoskeletal reorganization (Dickson, 2002; Pollard and Borisy, 2003). However, the components that guide the migration and cell extension of other cell types remain a mystery (Rorth, 2003).

Intriguingly, developing muscles in a variety of animals also extend plasma membrane in a regulated fashion. At the sites of incoming motor axons, muscle membrane extensions called microspikes or myopodia have been observed in *Drosophila* (Bate, 1990; Ritzenthaler et al., 2000), *Xenopus* (Kullberg et al., 1977), rat (Uhm et al., 2001) and mouse (Misgeld et al., 2002), and probably facilitate the development of the neuromuscular junction (NMJ). Mouse myopodia are enriched with clusters of acetylcholine receptors (AChRs) (Misgeld et al., 2002), whereas in rat, agrin can elicit the microspikes and mimic the effects of incoming axons (Uhm et al., 2001). Although agrin is well known to activate the MuSK receptor tyrosine kinase and thereby promote clustering of AChRs at the postsynaptic membrane (DeChiara et al., 1996; Gautam et al., 1996), it is unknown if agrin elicits muscle membrane extension through a similar signaling pathway.

The muscles of *C. elegans* also extend specialized plasma membrane to motor axons (Stretton, 1976; Sulston and Horvitz, 1977; White et al., 1986). In wild-type adult animals, there are 95 body wall muscles (BWMs) that are distributed along the length of the worm in four rows (Sulston and Horvitz, 1977; Sulston et al., 1983) (Fig. 1). There are two dorsal and two ventral BWM quadrants. The dorsal muscles extend membrane called muscle arms to the dorsal nerve cord, where muscle arm termini harbor the postsynaptic element of the NMJ (White et al., 1976). Similarly, ventral muscles extend arms to the ventral nerve cord and form NMJs (Fig. 1). Unlike microspikes or myopodia, muscle arms are retained after the formation of the NMJ and therefore provide a convenient model system for the genetic analysis of muscle membrane extension.

Although several lines of evidence suggest that muscle arms are guided to the nearest nerve cord (Hall and Hedgecock, 1991; Hedgecock et al., 1990), the nature of the guidance system is unknown. We and others suggest that there are two phases of muscle arm development (Dixon and Roy, 2005) (C. R. Norris, I. A. Bazykina, E. M. Hedgecock and D. H. Hall, personal communication). During embryogenesis, muscle arms probably arise through a passive process that is initiated by juxtaposition between the myoblast and the nascent motor axon. As the myoblast moves from the nerve cord, muscle membrane remains connected to the nerve cord, resulting in an embryonic muscle arm. By contrast, muscle arm extension during larval development is an active process that requires regulators of the actin cytoskeleton, including ADF/Cofilin (*unc-60B*) (Dixon and Roy, 2005). It is unknown if microspikes, myopodia, and muscle arms share common regulatory mechanisms.

Department of Medical Genetics and Microbiology, Donnelly Centre for Cellular and Biomolecular Research, University of Toronto, Toronto, ON, M5S 1A, Canada. [1]Collaborative Program in Developmental Biology, University of Toronto, Toronto, ON, M5S 1A8, Canada.

*Author for correspondence (e-mail: peter.roy@utoronto.ca)

Accepted 26 January 2006

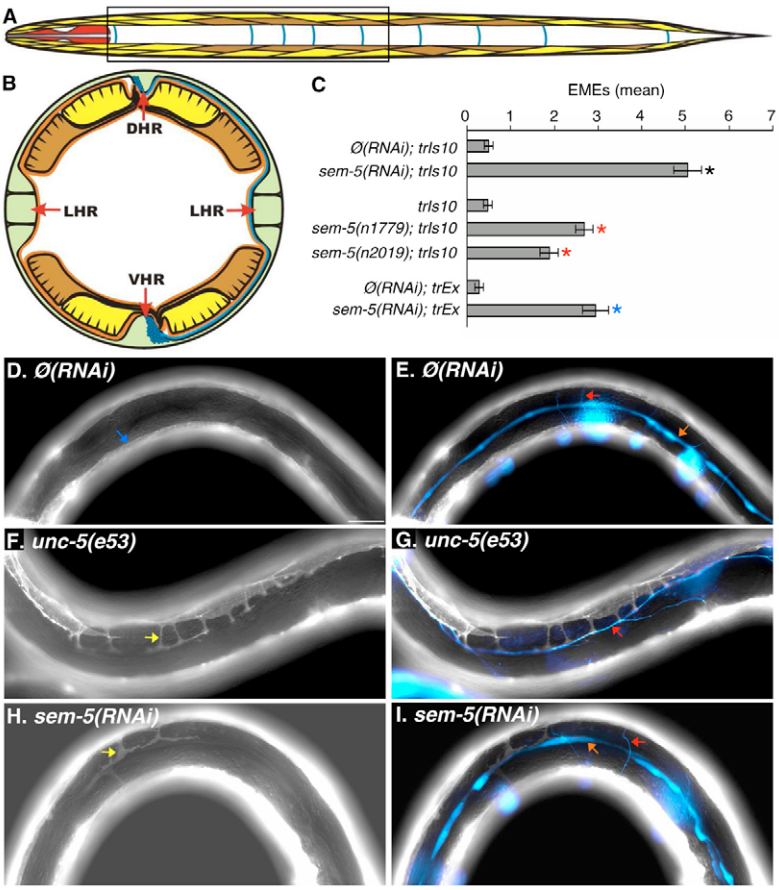

Fig. 1. Disruption of *sem-5* results in ectopic membrane protrusions (EMEs). (**A**) An illustration of the BWMs (yellow and brown) and DA and DB commissural motor neurons (blue) of the left side of *C. elegans*. Both the outer row (brown) and the inner row (yellow) of BWMs express Mb::YFP from the *trIs10* integrated array, whereas only select BWMs of the outer row (brown) express Mb::YFP from *trIs30*. The boxed area indicates the area of the worm seen in D-I. (**B**) A cross-section of A, with the dorsal, ventral and lateral hypodermal ridges (HR) indicated. (**C**) Disruption of *sem-5* by RNAi or hypomorphic loss-of-function mutations results in EMEs as visualized with *trIs10*, as does *sem-5(RNAi)* in the background of an different muscle reporter strain *RP168 [trEx(C26G2.1p::dsred2; B0285.6::mb::yfp)]* (Dixon and Roy, 2005), denoted as *trEx*. Colored asterisks indicate significant differences ($P<0.001$) versus the relevant controls: black, versus *trIs10;Ø(RNAi)*; red, versus *trIs10*; blue, versus *trEx;Ø(RNAi)*. $n>80$ for each genotype. Error bars represent the standard error of the mean (s.e.m.). (**D**,**E**) The lateral BWM membrane of *trIs10* worms fed upon *Ø(RNAi)* is not disrupted (blue arrow in D) and commissural motor axon guidance is normal (red arrow in E). The *unc-129nsp::cfp* promoter also drives expression of CFP in the hypodermal seam cells (orange arrows in E,I). (**F**,**G**) *trIs10; unc-5(e53)* worms extend muscle arms (yellow arrow in F) towards misguided motor axons (red arrow in G). (**H**,**I**) *trIs10; sem-5(RNAi)* worms show numerous EMEs (yellow arrow in H) but commissural axon guidance is normal (red arrow in I). Scale bar: 50 μm.

Here, we present results from two RNAi screens for genes required to regulate muscle membrane extension in *C. elegans*. In a small screen of 24 genes that guide other cell extensions and migrations in the worm, we found that disruptions in an FGF pathway result in ectopic membrane extensions (EMEs) from the BWMs. To find additional genes that regulate EMEs, we also screened 847 genes that result in an uncoordinated (Unc) or paralyzed (Prz) phenotype when targeted by RNAi (Kamath et al., 2003; Simmer et al., 2003). We reasoned that some of these behavioral phenotypes may result from defects in muscle membrane extension. Indeed, we found that several integin and laminin components not only have EMEs, but also have muscle arm extension defects (MADs) in which the larval muscle arms fail to extend. Our results are consistent with a model whereby integrins and laminins are needed for directed muscle arm extension to the nerve cords, while FGF signaling provides a general mechanism to regulate membrane extension.

MATERIALS AND METHODS

Constructs, nematode strains, transgenics, microscopy and muscle arm counts

All constructs used in this work are described in Table S2 in the supplementary material. Details of plasmid construction are available upon request. All strains used in this work are described in Table S3 in the supplementary material. Transgenic animals were generated using standard injection and integration techniques (Mello et al., 1991) and resulting integrants were back-crossed to N2 (wild-type) three times. For microscopy, worms were anesthetized in 2-10 mM Levamisole (Sigma) in M9 solution and mounted on a 2% agarose pad. All images were acquired with a Leica DMRA2 compound microscope equipped with a Retiga 1300 digital camera (Q imaging) using Open Lab (Improvision) software. Images were processed using Volocity (Improvison) and Adobe Photoshop 7.0 (Adobe Systems). All muscle arm counts were of the dorsal right-hand nerve cord. Unless otherwise indicated, all counts were of muscles 9-21 and performed in the background of RP247[*trIs30*], as described (Dixon and Roy, 2005).

The RNAi screen for EMEs, scoring the EME phenotype and statistical analysis

Twenty-four RNAi by feeding vectors targeting known cell migration guidance genes were constructed by inserting 0.8-1.5 kb fragments of genomic DNA isolated by PCR from exon-rich regions of each gene into the *Eco*RI site of the L4440 plasmid (Timmons and Fire, 1998). These vectors were transformed into HT115 bacteria (Timmons et al., 2001) using standard protocols. RNAi by feeding vectors targeting *let-60*, *ptp-2*, *soc-2*, *egl-15* and 14 other RTK genes (Table S1 in the supplementary material) and 847 Unc or Prz genes were from the Ahringer library (Kamath et al., 2003). A similar procedure was used for all RNAi-by-feeding experiments. L4-stage worms (the P_os) were first plated onto 6 cm MYOB-agar plates lacking food and allowed to run for ~0.5 hour to remove any contaminating OP50 bacteria. Then, for the screens of guidance and RTK genes, four worms were re-plated into a 6 cm NGM-RNAi-inducing agar dish containing a single RNAi-inducing bacterial clone. For the screen of 847 Unc or Prz genes two P_os were re-plated into separate RNAi-seeded wells of a 12-well dish. In both cases, after three days growth at 20°C, late L4 or young adult F1 progeny were scored for the EME phenotype (+/–) at the dissection microscope. Positive hits were re-tested and the EME phenotype was quantified by counting the number of individual membrane processes extending from the body wall muscles into the lateral hypodermal space. In each case, the side of the animal was noted. Equal numbers of the left and right hand sides were counted for each strain and averaged. All statistical analyses of muscle arm counts and EMEs were performed using Student's *t*-test for independent samples.

sem-5 and *egl-15* rescue and cell specific RNAi

The ability of *sem-5* to rescue the EME phenotype was tested by injecting *trIs10; sem-5(n1779)* worms with a construct directing the expression of *sem-5* genomic DNA (*sem-5g*) either in BWMs (*myo3p::sem-5g*) or pan-neuronally *(F25B3.3p::sem-5g)*. The presence of the rescuing arrays were followed in the BWMs and nervous system with the co-injection reporters *myo-3p::cfp* and *F23B3.3::dsred2*, respectively. Control strains contain the co-injection markers plus pBluescript (Stratagene) DNA. The ability of *egl-15* to rescue the EME phenotype in muscle was tested by injecting *trIs10; egl-15(n484)* worms with a construct directing the expression of *egl-15(5A)* cDNA (courtesy of O. Hobert) from the *myo-3* promoter. The presence of the rescuing arrays was followed with the co-injection reporter *myo-3p::cfp*. A control line was also generated using the same concentration of pBluescipt instead of *myo3p::egl-15(5A)*^{cDNA}. We also generated worms with an *Ex* array directing the production of Mb::YFP in the BWM in the background of *oxIs14; egl-15(n484); otEx1270* and *oxIs14; egl-15(n484); otEx1269* (Bulow et al., 2004). These *otEx* arrays drive expression of EGL-15A in the hypodermis from the *dpy-7* promoter and rescue the axon defects of *egl-15(n484)* (Bulow et al., 2004). As a negative control, cousins lacking the *otEx* arrays were also counted. Before counting EMEs, we selected animals that brightly fluoresced in the co-injection fluorescent channels to ensure that animals carried the extra-chromosomal array in many of their cells.

Constructs directing the BWM-specific expression of dsRNA against *gfp*, *unc-115*, *sem-5* and *egl-15* gene products were generated by subcloning a coding-rich genomic fragment for each gene into the *pPRSD102* plasmid, a derivative of *pPD95.86* that contains an expanded MCS 3′ to the *myo-3* promoter, and isolating clones for *gfp*, *unc-115*, *sem-5* and *egl-15* fragments in both orientations with respect to the *myo-3* promoter. To target *mb::yfp* mRNA for degradation, for example, two plasmids directing the production of RNA in opposite directions are co-injected along with the plasmid directing expression of a DsRed2 in BWMs to mark the array. All cell specific RNAi experiments were performed in a *trIs10; sid-1(qt9)* background. Multiple transgenic lines were isolated from each injection and from these lines, those worms that displayed robust expression of the co-injection marker in the body wall muscles were scored for EMEs.

Time-course data collection

Embryos from *trIs10; egl-15(n484)* and *trIs10; sos-1(cs41)* worms were raised at either 20°C (for up-shift experiments) or 25°C (for downshift experiments) for 12 hours, then harvested at room temperature using the hypochlorite method and plated onto MYOB agar plates lacking food (Lewis and Fleming, 1995). The eggs were allowed to hatch overnight at either 20°C or 25°C without food, causing them to arrest as L1 hatchlings. The next day, the synchronized L1 population was divided and transferred to seven different plates and stored at either 20°C or 25°C (the 0 hour time point). Individual plates were transferred between 20°C and 25°C incubators when appropriate. For example, in *trIs10; egl-15(n484)* up-shift experiments, one plate containing L1s harvested and synchronized at 20°C was transferred to 25°C after 6 hours (the 6 hour time point), another plate transferred to 25°C after 12 hours (the 12-hour time point), etc. All strains were scored for the EME phenotype upon reaching young adulthood.

let-756 rescue and mosaic analysis

let-756 rescue was tested using various promoters that drive *let-756* expression in different cell types. RP175 and RP176 are two independent lines of the same genotype *Ex[pPRRF186(let-756p::YFP); (pPRRF187(let-756p::LET-756)]; let-756(s2887) unc-32(e189)III* that were used in a mosaic analysis to determine where *let-756* expression was required to rescue the lethality conferred by *let-756(s2887)*. Both RP175 and RP176 depend on the *Ex* array for viability, as no non-fluorescent animals are ever observed in these two strains (n>1000). We collected 47 RP175 and 95 RP176 animals that were dramatically mosaic for the *Ex* array, being present in only a few *let-756*-expressing cells. Of these, 10 RP175 animals had YFP expression exclusively in the BWMs, five had YFP expression exclusively in the pharynx and one had expression in only one CAN neuron. For RP176, 23 animals had YFP expression exclusively in the BWMs, seven had YFP expression exclusively in the pharynx and five had expression in only one or two CAN neurons. We found no RP175 or RP176 animals with YFP expression in only the G1 and G2 glandular cells or only in the intestine.

RESULTS

sem-5 negatively regulates membrane protrusion from the body wall muscles

To identify genes required to regulate muscle plasma membrane extension, we first built a strain called RP1 that expresses a membrane-anchored YFP (Mb::YFP) (Dixon and Roy, 2005) in all BWMs from a transgenic array called *trIs10* (Fig. 1). Because BWMs of the dorsal quadrants extend muscle arms to the dorsal cord, and the ventral BWMs extend muscle arms to the ventral cord (Dixon and Roy, 2005; Hedgecock et al., 1990; White et al., 1986), the left and right lateral hypodermal ridges are devoid of BWM membrane extensions in wild-type animals (Fig. 1). We therefore expected that any EMEs projecting into the lateral space as a result of disrupted plasma membrane extension would be readily visible in living RP1 animals. To test this, we examined the plasma membrane of BWMs in *unc-5* mutants. In *unc-5* mutants, commissural motor axons fail to extend to the dorsal cord and instead extend longitudinally along the lateral and ventral hypodermal ridges (Hedgecock et al., 1990). Muscle arms from dorsal BWMs extend to these errant lateral and ventral motor axons as a secondary consequence (Hedgecock et al., 1990). As expected, muscle arms that extend to the misguided axons are readily visible in *trIs10; unc-5(e53)* animals (Fig. 1), demonstrating that *trIs10* enables the visualization of BWM membrane in the lateral hypodermal space.

We next investigated if genes required for the guidance of cell extensions and migrations might also play a role in regulating BWM membrane extension. Twenty-four genes required for guidance were targeted in an RNAi pilot screen using RP1 worms (see Materials and methods and Table S1 in the supplementary material). *sem-5*, which encodes a small adapter protein that is orthologous to Grb2 and functions downstream of receptor tyrosine kinases (Borland et al., 2001; Clark et al., 1992; Moghal and Sternberg, 2003; Stern et al., 1993), was the only RNAi target that resulted in EMEs (Fig. 1). Two *sem-5* hypomorphs, *n1779* and *n2019*, both have significantly more EMEs than the reporter strain alone (P<0.001, Fig. 1C), confirming that disruption of *sem-5* results in the EME phenotype. We also observe EMEs in *sem-5(RNAi)* animals in a reporter strain that expresses DsRed2 throughout the BWMs, demonstrating that the EME phenotype is independent of the Mb::YFP reporter (Fig. 1C). Furthermore, *sem-5(RNAi)* does not induce EMEs in all cells, as the plasma membrane of the seam cells and DA and DB motoneurons in animals treated with *sem-5(RNAi)* do not exhibit EMEs (n=100 animals, see Fig. S1 in the supplementary material). These results suggest that *sem-5* is required to prevent ectopic membrane extensions from the BWMs.

The EMEs revealed by *sem-5* hypomorphic activity often resemble the misguided muscle arms in mutants such as *unc-5(e53)*. However, three lines of evidence suggest that EMEs are not a secondary consequence of misguided axons as in *unc-5* mutants. First, the morphology and position of the DA, DB, DD and VD commissural motor axons in *sem-5(RNAi)*-treated RP1 animals is wild type (Fig. 1H,I). Second, disruption of *sem-5* by RNAi in worms expressing a fluorescent reporter in all neurons (see Table S3 in the supplementary material) does not produce lateral axon guidance defects (n=10 animals). Third, EMEs do not extend to any particular lateral axon (data not shown), making it unlikely that

EMEs extend into the lateral space because of altered lateral neuron fate. Together these results suggest that EMEs are not a secondary consequence of defects in neuronal development.

sem-5 expression in BWMs is both necessary and sufficient to prevent EMEs

To determine where *sem-5* is required to regulate membrane extension from the BWMs, we first examined the cells that express a YFP reporter from ~3.0 kb of promoter and enhancer sequences of *sem-5*. Animals carrying this transgene express YFP in many cells throughout development and in the adult, including the vulval precursor cells, hypodermis, intestine, neurons and the BWMs (see Fig. S2 in the supplementary material). To test if *sem-5* expression in muscles is sufficient to prevent the EME phenotype, we built a construct designed to express SEM-5 specifically in muscle cells from the *myo-3* promoter (*myo-3p*::SEM-5) (Okkema et al., 1993). Three independent transgenic lines containing *myo-3p*::SEM-5 were isolated in the background of the *sem-5(n1779)* hypomorphic mutation. Each line displayed significantly fewer EMEs than the negative control ($P<0.001$, Table 1). By contrast, pan-neuronal expression of SEM-5 does not rescue the EME phenotype (Table 1). These results show that *sem-5* expression in muscle is sufficient to rescue the EME phenotype.

To investigate if *sem-5* expression in BWMs is necessary to prevent EMEs, we developed an approach to knock down gene expression in a BWM-specific manner. We built constructs designed to express double-stranded RNA sequence (dsRNA) corresponding to the coding sequence of the targeted gene specifically in the muscles. To prevent the systemic distribution of the muscle-expressed dsRNA (Fire et al., 1998) and limit the RNAi effect to the muscles, we expressed the dsRNA in the background of a *sid-1(qt9)*-null mutant (a kind gift from Craig Hunter). SID-1 is required for dsRNA uptake into cells (Feinberg and Hunter, 2003; Winston et al., 2002). Therefore the RNAi effect should be limited to the BWMs that express the dsRNA. To test this approach, we injected *trIs10; sid-1(qt9)* animals with three transgenes: two that direct the production of dsRNA against *gfp* and a third that expresses nuclear-localized DsRed2 in muscle to mark the presence of the extra-chromosomal (Ex) array that contains the transgenes. We expected that YFP expression would be knocked down in muscles that have the Ex array because *gfp*-coding sequence is 99% identical to *yfp*, while neighboring muscles that do not have the Ex array should maintain YFP expression. In *trIs10; sid-1(qt9)* animals mosaic for the Ex array, 94% of DsRed2(+) BWMs were YFP(–) (n=143), while 99% of DsRed2(–) BWMs were YFP(+) (n=79) (Fig. 2A). Conversely, in *trIs10; sid-1(qt9)* lines expressing dsRNA in BWMs targeting *unc-115*, which is not expressed in muscles (Lundquist et al., 1998) and the sequence of which is unrelated to *gfp*, 100% of DsRed2(+) BWMs were YFP(+) (n=201) (Fig. 2B). These results demonstrate that the RNAi effect can be restricted to a cell of interest through the cell-specific expression of *dsRNA* in the background of a *sid-1* null mutation.

To determine if *sem-5* expression in the BWMs was necessary to prevent EMEs, we isolated four independent lines of *trIs10; sid-1(qt9)* animals expressing *sem-5(dsRNA)* specifically in BWMs and found that each had significantly more EMEs than negative controls (Fig. 2). Together, our results suggest that *sem-5* expression in BWMs is both necessary and sufficient to negatively regulate ectopic membrane extension from the BWMs.

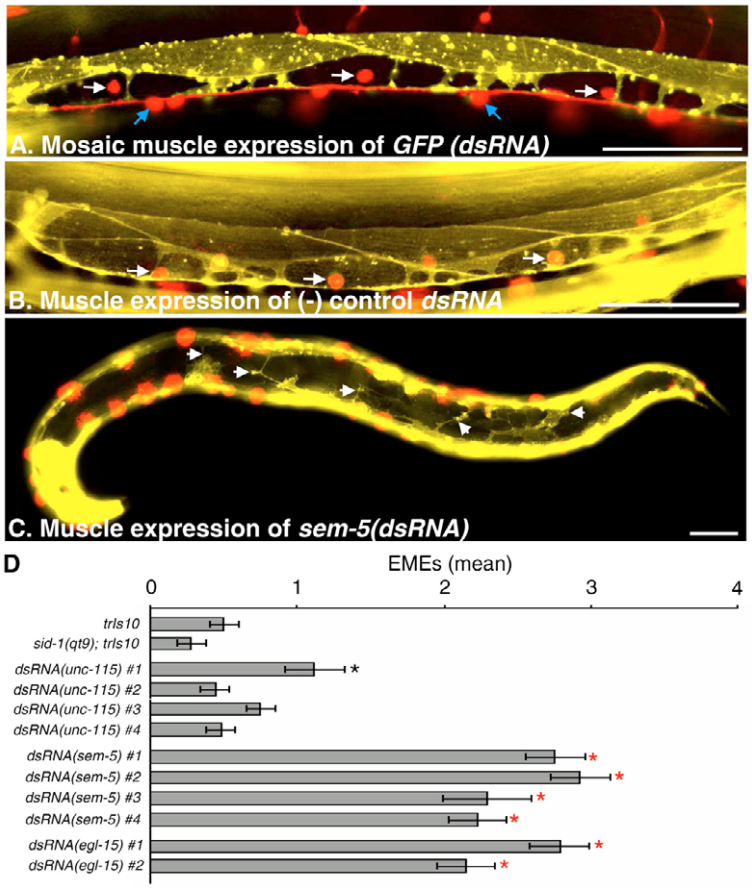

Fig. 2. *sem-5* expression in BWMs is necessary to prevent EMEs. (**A**) In a *trIs10 I; sid-1(qt9) V; Ex(myo-3p::gfp(fRNA); myo-3p::gfp(rRNA); myo-3p::NLS::DsRed)* background, BWM cells that are positive (NLS::DsRed2, white arrows) for the extra-chromosomal array directing the production of dsRNA targeting *gfp* do not produce Mb::YFP. Blue arrows indicate DsRed2-positive nuclei of ventral cord motoneurons. The expression of DsRed2 in these cells is from the *trIs10* transgene, not the extra-chromosomal array. (**B**) A negative control expressing dsRNA targeting *unc-115*. White arrows indicate BWM cells that express NLS::dsRed2 and therefore are positive for the extra-chromosomal array. YFP expression in the BWMs is retained. (**C**) Expression of dsRNA targeting *sem-5* in BWM results in numerous EMEs (white arrows). (**D**) Quantification of the EME phenotype in four lines (1-4) of *unc-115(dsRNA)* worms, four lines (1-4) of *sem-5(dsRNA)* worms and two lines (1 and 2) of *egl-15(dsRNA)* worms. Except for the *trIs10* control, all strains are in the *trIs10*; *sid-1(qt9)*-null background. The full genotype of each strain can be found in Table S3 in the supplementary material. Red asterisks indicate statistical significance at the $P<0.001$ level versus the *sid-1(qt9); trIs10* negative control. $n>30$ for all genotypes and error bars represent the s.e.m. The black asterisk indicates that one of the control lines displayed significantly more EMEs than the other three control lines. Scale bars: 50 μm.

Table 1. Disruption of the FGF pathway in BWMs results in EMEs

	Genotype*	Description	*n*	EMEs†	*P* value‡	*P* value‡
Compromised FGF signaling results in EMEs						
1	*Ø(RNAi)*	Wild type	204	0.6±0.9	–	–
2	*sem-5(RNAi)*	Grb2 adapter	68	5.1±2.5	<0.001 (1)	–
3	*egl-15(RNAi)*	FGF receptor	42	4.1±2.5	<0.001 (1)	–
4	*let-60(RNAi)*	Ras GTPase	86	4.0±2.1	<0.001 (1)	–
5	*soc-2(RNAi)*	Ras adapter protein	42	3.9±3.0	<0.001 (1)	–
6	*ptp-2(RNAi)*	Tyrosine phosphatase	88	1.9±1.5	<0.001 (1)	–
7	*trIs10*	Wild type	244	0.5±0.8	–	–
8	*trIs10* 25°C	Wild type	88	0.8±1.2	–	–
9	*let-756(s2613)*	FGF-9 ligand (hypomorph)	86	3.4±1.8	<0.001 (7)	–
10	*egl-17(n1377)*	FGF ligand (null)	84	0.6±0.9	>0.05 (7)	–
11	*egl-15(n1477)*	FGF receptor (hypomorph)	84	4.3±2.4	<0.001 (7)	–
12	*egl-15(n1783)*	FGF receptor (hypomorph)	88	2.7±2.4	<0.001 (7)	–
13	*egl-15(n484ts)*	FGF receptor (hypomorph)	88	1.2±1.5	<0.001 (7)	–
14	*egl-15(n484ts)* 25°C	FGF receptor (hypomorph)	88	4.2±3.5	<0.001 (8)	–
15	*soc-1(n1789)*	Gab-1 adapter protein	86	3.0±1.7	<0.001 (7)	–
16	*sos-1(cs41ts)*	SOS Ras-GEF (hypomorph)	86	1.5±1.9	<0.001 (7)	–
17	*sos-1(cs41ts)* 25°C	SOS Ras-GEF (hypomorph)	86	6.0±4.0	<0.001 (8)	–
18	*let-60(n2021)*	Ras GTPase (hypomorph)	88	1.6±1.7	<0.001 (7)	–
***sem-5* expression in the BWMs, but not the nervous system, rescues the EME phenotype**						
19	*sem-5(n1779); Ex(myo3p::cfp)*	Control for rows 20-22 below	69	3.3±1.9	–	–
20	*sem-5(n1779); Ex(myo3p::sem-5g; myo3p::cfp)*	BWM SEM-5 expression line #1	82	1.1±1.1	<0.001 (19)	–
21	*sem-5(n1779); Ex(myo3p::sem-5g; myo3p::cfp)*	BWM SEM-5 expression line #2	49	0.8±1.0	<0.001 (19)	–
22	*sem-5(n1779); Ex(myo3p::sem-5g; myo3p::cfp)*	BWM SEM-5 expression line #3	29	1.0±1.0	<0.001 (19)	–
23	*sem-5(n1779); trEx(f25b3.3p::dsred)*	Control for rows 24-26 below	27	3.4±2.4	–	–
24	*sem-5(n1779); Ex(f25b3.3p::sem-5g;; f25b3.3p::dsred)*	Pan-neuronal SEM-5 expression line #1	49	3.0±2.4	>0.05 (23)	–
25	*sem-5(n1779); Ex(f25b3.3p::sem-5g;; f25b3.3p::dsred)*	Pan-neuronal SEM-5 expression line #2	33	3.1±1.7	>0.05 (23)	–
26	*sem-5(n1779); Ex(f25b3.3p::sem-5g;; f25b3.3p::dsred)*	Pan-neuronal SEM-5 expression line #3	46	2.9±2.6	>0.05 (23)	–
***egl-15(5A)^{cDNA}* expression in the BWMs, but not the hypodermis, rescues the EME phenotype**						
27	*egl-15(n484); Ex(myo3p::cfp)* 25°C	Control for rows 28-31 below	50	7.2±2.7	–	–
28	*egl-15(n484); Ex(myo3p::egl-15(5A)^{cDNA}; myo3p::cfp)* 25°C	BWM EGL-15(5A) expression line #1	40	3.6±3.2	<0.001 (27)	–
29	*egl-15(n484); Ex(myo3p::egl-15(5A)^{cDNA}; myo3p::cfp)* 25°C	BWM EGL-15(5A) expression line #2	34	3.6±3.1	<0.001 (27)	–
30	*egl-15(n484); Ex(myo3p::egl-15(5A)^{cDNA}; myo3p::cfp)* 25°C	BWM EGL-15(5A) expression line #3	54	3.6±2.4	<0.001 (27)	–
31	*egl-15(n484); Ex(myo3p::egl-15(5A)^{cDNA}; myo3p::cfp)* 25°C	BWM EGL-15(5A) expression line #4	34	5.5±3.3	<0.05 (27)	–
32	*egl-15(n484); Ex(myo3p::mb::yfp); oyIs14* 25°C	Control for row 33 below	44	2.2±1.5	–	–
33	*egl-15(n484); Ex(myo3p::mb::yfp); oyIs14; otEx1270* 25°C	Hypodermal EGL-15(5A) expression	50	2.3±1.5	>0.05 (32)	–
34	*egl-15(n484); Ex(myo3p::mb::yfp); oyIs14* 25°C	Control for row 35 below	44	2.5±1.6	–	–
35	*egl-15(n484); Ex(myo3p::mb::yfp); oyIs14; otEx1269* 25°C	Hypodermal EGL-15(5A) expression	36	3.1±1.7	>0.05 (34)	–
***clr-1* loss of function and *let-60* gain of function suppresses the EME phenotype in *sem-5* and *egl-15* reduction of function mutants**						
36	*clr-1(e1745ts)* 15°C	RPTP (hypomorph)	80	0.5±0.8	>0.05 (7)	–
37	*clr-1(e1745ts)*	RPTP (hypomorph)	88	0.4±0.7	>0.05 (7)	–
38	*clr-1(e1745ts); sem-5(RNAi)*		28	0.7±0.9	<0.001 (2)	>0.05 (7)
39	*clr-1(e1745ts); egl-15(RNAi)*		44	1.2±1.2	<0.001 (3)	<0.001 (7)
40	*let-60(n1046)*	Ras GTPase (hypermorph)	44	0.5±0.9	>0.05 (7)	–
41	*let-60(n1046); sem-5(RNAi)*		88	1.2±1.3	<0.001 (2)	<0.001 (40)
42	*let-60(n1046); egl-15(RNAi)*		74	1.0±1.0	<0.001 (3)	<0.001 (40)

*The *trIs10* array was used in all strains to visualize muscle plasma membrane, except the strains in rows 32-35 in which an extra-chromosomal array *Ex(myo-3p::Mb::YFP)* was used instead, accounting for the lower number of EMEs (see Materials and methods for more details). *otEx1270* and *otEx1269* express the EGL-15(5A) isoform specifically within the hypodermis from the *dpy-7* promoter (Bulow et al., 2004). *oxIs14* is a *sra-6p*::GFP reporter and is not relevant to this study. All counts used late L4 or young adult worms from mixed-stage populations, except lines 27-35 where L1s were picked at 20°C and then allowed to develop to adulthood at 25°C. As shown in Fig. 4, this treatment ensures that in all worms subsequently counted *egl-15* activity is lost during the crucial temperature sensitive period. The lower EME count in *egl-15(n484); trIs10* worms reported in line 14 probably reflects the fact that these worms were derived from a mixed-stage population that was shifted from 20°C to 25°C and therefore contained some animals past the TSP. All counts were performed on worms maintained at 20°C, unless otherwise indicated.

†All counts represent the mean±s.d.

‡*P* values derived from Student's *t*-test with respect to the appropriate negative control (comparison row indicated in brackets).

An FGF pathway prevents EMEs during larval development

SEM-5 and its mammalian ortholog Grb2 can function as adaptor proteins linking ligand-bound receptor tyrosine kinases (RTKs) to the guanine nucleotide exchange factor SOS that activates Ras within the cell (Lowenstein et al., 1992; Moghal and Sternberg, 2003; Stern et al., 1993). To determine if *sem-5* regulates muscle membrane protrusions downstream of an RTK, we screened 14 *C. elegans* RTKs genes for the EME phenotype using RNAi (see Table S1 in the supplementary material). *egl-15*, which encodes the lone FGF receptor (FGFR) in *C. elegans* (DeVore et al., 1995), was the only RTK that resulted in the EME phenotype (Table 1). Three *egl-15* hypomorphic alleles that we examined also have EMEs (Fig. 3A,B, Table 1). Although BWM spatial expression of *egl-15* has not yet been reported, both SAGE analysis and Affymetrix microarray analysis of cultured *C. elegans* myoblasts reveals low, but significant, expression of *egl-15* mRNAs (Don Moerman and David Miller, III, personal communication). Knocking down *egl-15* activity specifically in BWMs using the same RNAi approach outlined above for *sem-5* results in significantly more EMEs than control strains (Fig. 2D). Moreover, a construct directing the expression of an *egl-15* cDNA from the *myo-3* promoter in the BWM rescues the EME phenotype of *trIs10; egl-15(n484)* worms (Table 1). Conversely, expression of *egl-15* in the hypodermis does not rescue the EME phenotype (Table 1, lines 32-35). These results suggest that FGFR activity within the BWMs is required to prevent the EME phenotype.

We next tested if other known FGF pathway genes play a role in regulating membrane extension from the BWMs. There are two putative FGF ligands upstream of *egl-15* encoded by *egl-17* (Burdine et al., 1997) and *let-756* (Roubin et al., 1999). The number of EMEs in *egl-17(n1377)* null animals did not differ from negative controls ($P>0.05$). By contrast, *let-756(s2613)* hypomorphs had significant numbers of EMEs ($P<0.001$) (Fig. 3C, Table 1), suggesting that

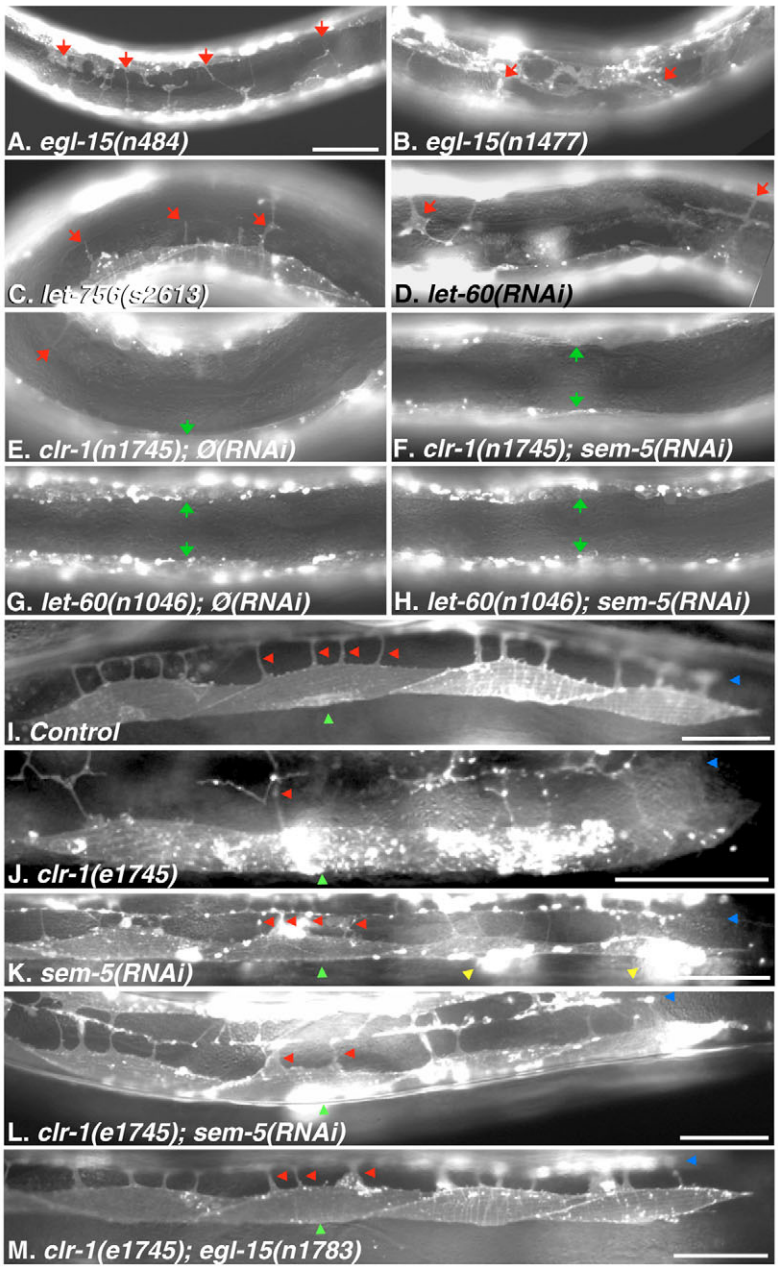

Fig. 3. An FGF pathway regulates muscle membrane extension. (**A-D**) Disruption of *egl-15*, *let-756* and *let-60* results in numerous EMEs. (**E-H**) The EMEs of *sem-5(RNAi)* worms (see Fig. 1H) are suppressed by *clr-1(e1745)* loss of function and *let-60(n1046)* gain of function, neither of which displays significant EMEs on their own. (A-H) Red arrows indicate individual EMEs, green arrows indicate intact lateral BWM membranes. (**I-M**) A dorsal right-hand side view of adult worms, showing BWMs numbers 9, 11, 13 (green arrowhead) and 15 [right to left, according to our numbering scheme (Dixon and Roy, 2005)], extending muscle arms (red arrowheads) to the dorsal nerve cord (blue arrowheads). (J) *clr-1(e1745); trIs30* worms extend significantly fewer muscle arms to the nerve cord than do controls. (K) *sem-5(RNAi); trIs30* worms extend muscle arms normally and display EMEs (yellow arrowheads). (L,M) The MAD phenotype of *clr-1(e1745)* worms is partially rescued in the background of *sem-5(RNAi)* (L) and fully rescued in the background of *egl-15(n1783)* (M). Scale bar: in A, 50 μm for A-H; in I-M, 50 μm.

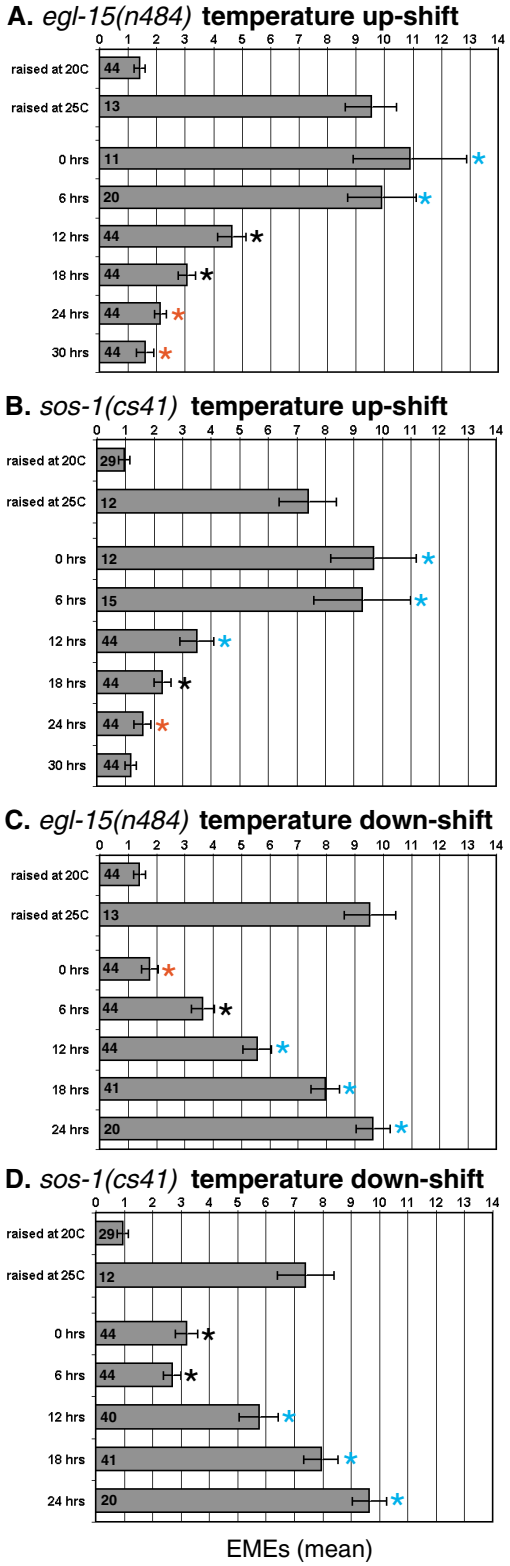

Fig. 4. Temperature-shift time-course experiments with temperature-sensitive alleles of FGF pathway components. (**A**) Synchronized *egl-15(n484); trIs10* L1 hatchlings that were raised at 20°C were either kept at 20°C or shifted to 25°C as hatchlings (0 hours), or 6, 12, 18, 24 or 30 hours after hatching. The number of EMEs was counted in these animals upon reaching young adulthood. The number of EMEs in *egl-15(n484); trIs10* animals raised at 25°C is also shown. A blue asterisks indicates that the number of EMEs is significantly greater than those in animals raised at 20°C ($P<0.001$). A black asterisks indicates that the number of EMEs is significantly different compared to animals raised at both temperatures ($P<0.001$). A red asterisks indicates that the number of EMEs is significantly lower compared to animals raised at 25°C ($P<0.001$). The number of animals counted is shown at the base of each bar. Error bars represent the s.e.m. (**B**) Synchronized *trIs10; sos-1(cs41)* hatchling L1s that were raised at 20°C were either kept at 20°C or shifted to 25°C as hatchlings (0 hours), or 6, 12, 18, 24 or 30 hours after hatching. (**C**) Synchronized *egl-15(n484); trIs10* hatchling L1s that were raised at 25°C were either kept at 25°C or shifted to 20°C as hatchlings (0 hours), or 6, 12, 18 or 24 hours after hatching. (**D**) Synchronized *sos-1(cs41); trIs10* hatchling L1s that were raised at 25°C were either kept at 25°C or shifted to 20°C as hatchlings (0 hours), or 6, 12, 18 or 24 hours after hatching. For B-D, the notation on the chart is the same as that in A.

LET-756 is the ligand necessary to prevent EME formation. Numerous genes function downstream of *egl-15*, including the adapter proteins *sem-5*(Grb2), *soc-1*(Gab1) and *soc-2*(Shoc-2/Sur-8), the non-receptor tyrosine phosphatase *ptp-2*(Shp2), the Ras guanine nucleotide exchange factor *sos-1* (Son of Sevenless), and the Ras-family GTPase *let-60* (Ras) (Borland et al., 2001). We determined that *soc-2(RNAi)*, *ptp-2(RNAi)* and *let-60(RNAi)* each induced EMEs (Fig. 3D, Table 1). EMEs were also observed in strains containing *soc-1*, *sos-1* and *let-60* hypomorphic alleles (Table 1). Together, these data suggest that FGF signaling negatively regulates ectopic membrane extensions from the BWMs.

To determine when FGF signaling is required to prevent EMEs, we performed temperature shift experiments using temperature-sensitive alleles of *egl-15(n484)* (Goodman et al., 2003) and *sos-1(cs41)* (Rocheleau et al., 2002) (see Fig. 4 and Materials and methods for details). Both *egl-15(n484)* and *sos-1(cs41)* worms shifted to 25°C before the third larval stage had more EMEs than the negative control animals kept at 20°C, while those shifted after the third larval stage did not (Fig. 4A,B). Conversely, mutant L1 hatchlings raised at 25°C and then immediately shifted to 20°C for the remainder of larval development show no more EMEs than animals raised continuously at 20°C (Fig. 4C,D), indicating that the FGF pathway is not required during embryogenesis to regulate EMEs. The number of EMEs in animals left in the non-permissive temperature significantly increased at each successive time point until the middle of the third larval stage at the 24 hour time point, when the number of EMEs was not different than animals raised constitutively at 25°C. These results show that FGFR signaling is required specifically during early to mid larval development to prevent EME formation. Larval muscle arm extension occurs exclusively during this same period (Dixon and Roy, 2005), suggesting that the FGF pathway functions to prevent widespread ectopic extension of the muscle membrane during this crucial period.

To investigate the effects of upregulation of the FGF pathway on membrane extension, we examined BWM plasma membrane in a *clr-1* loss-of-function mutant. *clr-1* encodes a BWM-expressed receptor tyrosine phosphatase that negatively regulates EGL-15 activity (Kokel et al., 1998). The *clr-1(e1745)* temperature-sensitive allele can suppress the EMEs induced by *egl-15* and *sem-5* hypomorphic activity (Fig. 3E,F, Table 1), consistent with the role of CLR-1 in antagonizing ELG-15-mediated signaling. Similarly, the *let-60(n1046)* hypermorph is able to partially suppress the EME

Table 2. Quantification of the MAD phenotype in FGF, ECM and adhesion mutants

	Genotype*	Description	*n*	MAs†	*P* value‡	*P* value‡
1	*Ø(RNAi)*	Wild type	15	3.6±0.9	–	–
2	*trIs30*	Control integrated array strain	15	3.3±1.0	–	–
3	*trEx*	Control extrachromosomal array strain	15	3.7±0.9	–	–
4	*clr-1(e1745)*	RPTP (hypomorph)	15	1.9±1.1	<0.001 (2)	–
5	*sem-5(RNAi)*	Grb2 adapter	15	3.3±1.1	<0.05 (1)	>0.05 (2)**
6	*clr-1(e1745);sem-5(RNAi)*		10	2.4±1.0	<0.001 (2)	<0.005 (4)
7	*clr-1(e1745);egl-15(n1783)*		15	3.7±0.8	>0.05 (3)	<0.001 (4)
8	*lam-1(RNAi)*	β-Laminin	15	2.6±1.1	<0.001 (1)	–
9	*lam-2(RNAi)*	γ-Laminin	15	2.3±1.1§	<0.001 (1)	–
10	*epi-1(RNAi)*	αB-laminin	15	2.6±1.0§	<0.001 (1)	–
11	*pat-2(RNAi)*	α-Integrin	15	1.8±1.0§	<0.001 (1)	–
12	*lam-1(rh219)*	β-Laminin (hypomorph)	15	2.6±1.6	<0.001 (2)	–
13	*unc-52(e998)*	Perlecan (hypomorph)	15	1.9±0.8§	<0.001 (2)	–

*The *trIs30* background was used for all counts, except line 3, where the strain counted is RP275 *trEx[him-4p::mb::yfp; hmr-1b::dsred2]* and line 8, where the strain counted is RP439 *clr-1(e1745); egl-15(n1783); trEx[him-4p::mb::yfp; hmr-1b::dsred2]*. Unless otherwise indicated all counts used late L4 or young adult worms from mixed-stage populations maintained at 20°C.
†All muscle arm (MA) counts represent the mean±s.d. for muscles 9-21 according to our published scheme (Dixon and Roy, 2005) except those denoted by §, which are of BWMs 9-15 only and which, for the purposes of statistical analysis, are compared with muscles 9-15 only in the appropriate negative control.
‡*P* values derived from Student's *t*-test with respect to the appropriate negative control (comparison row indicated in brackets). ***sem-5(RNAi)* treatment in line 6 results in a small reduction in muscle arm number compared with *trIs30; Ø(RNAi)* but not compared with the parent *trIs30* strain alone.

phenotype induced by *sem-5(RNAi)* and *egl-15(RNAi)* (Fig. 3G,H; Table 1). These data are consistent with previous work showing that *let-60* functions in the FGF pathway, but does not mediate all aspects of EGL-15 function (DeVore et al., 1995; Sundaram et al., 1996).

Interestingly, *clr-1(e1745)* mutants have a dramatic reduction in the number of muscle arms compared with controls (Fig. 3I,J, Table 2), suggesting that larval muscle arms fail to extend in these mutants (Dixon and Roy, 2005). The MAD phenotype of *clr-1* mutants is partially suppressed by *sem-5(RNAi)* and completely suppressed in an *egl-15(n1783)* background (Fig. 3L,M, Table 2). These results suggest that the level of EGL-15 activity is a key determinant of the ability of the BWM to extend plasma membrane: decreased EGL-15 activity results in ectopic membrane extensions, while increased EGL-15 activity abrogates larval muscle arm extension.

LET-756 restricts EMEs non-autonomously

To understand better how *let-756* restricts ectopic muscle membrane extensions, we first examined the *let-756* expression pattern using *let-756* promoter and enhancer sequence (*let-756p*) to drive YFP expression. Worms transgenic for *let-756p::YFP* express YFP in the BWMs, the pharynx, the CAN neuron and two unidentified neurons of the head as previously described (Bulow et al., 2004; Popovici et al., 2004) (see Fig. S2 in the supplementary material). Although the same cells expressed a LET-756::YFP fusion protein driven from the *let-756p*, we also observed nuclear localization of LET-756::YFP, along with pericellular expression around the BWMs that is very similar to that of CLR-1 (Kokel et al., 1998) (Fig. 5A-D).

We rescued the lethal phenotype of *let-756(s2887)* null mutants with an extra-chromosomal array that contained both the *let-756p::*YFP reporter and a second construct that used the same *let-756p* to drive the expression of *let-756* genomic coding sequence. Using the *let-756p::*YFP reporter to mark the cells that expressed LET-756 from the rescuing array, we determined that LET-756 expression in a single CAN neuron, a single BWM or cells in the pharynx was sufficient to rescue the lethality of *let-756(s2887)* nulls. Importantly, we could find no *let-756(s2887)* homozygotes that did not express YFP (n>1000), indicating that physiologically relevant LET-756 is not expressed in cells that do not also express YFP from the array. Moreover, when only a small number of BWMs or pharynx cells had the rescuing array in *let-756(s2887)* homozygotes, the animal had a pronounced bulge near the site of YFP expression, suggesting local rescue of the scrawny phenotype (Fig. 5E,F). Together, our observations demonstrate that transgenic expression of *let-756* from any one of a number of distinct cell types is sufficient to rescue the lethal phenotype of *let-756* nulls.

As *let-756* expression from distinct cell types rescued the lethal phenotype of *let-756* nulls, we tested if the same was true for the EME phenotype. We observed complete rescue of both lethality and EMEs in *let-756(s2887)* nulls expressing LET-756 from the endogenous *let-756p*, in neurons from the pan-neuronal *F25B3.3* promoter or in the hypodermis from the *dpy-7* promoter (Fig. 5G). This suggests that LET-756 functions non-autonomously to negatively regulate EMEs from the body wall muscles.

Disruptions of integrin and laminin result in both EMEs and MADs

Postsynaptic termini of the neuromuscular junction reside on the distal ends of muscle arms (Dixon and Roy, 2005; Stretton, 1976; Sulston and Horvitz, 1977; White et al., 1986). We reasoned that disruption of muscle arm extension might therefore result in locomotory defects. In an effort to identify additional genes that regulate muscle membrane extension, we screened 847 genes that result in an uncoordinated or paralyzed phenotype when targeted by RNAi (Kamath and Ahringer, 2003; Simmer et al., 2003), 23 of which resulted in a strong EME or MAD phenotype (M.A., R.F., S.J.D. and P.J.R., unpublished). One of these genes, *lam-1*, encodes the only laminin β-subunit in *C. elegans* (Huang et al., 2003; Hutter et al., 2000) and results in significant EMEs when disrupted by RNAi or mutation (Fig. 6, Table 3). *pat-4*, which encodes an integrin-linked kinase ortholog (Mackinnon et al., 2002), and *pat-6*, which is required for the assembly of integrin complexes (Lin et al., 2003), were also identified in our screen (Table 3). These results prompted us to investigate other integrin and laminin genes (Cox and Hardin, 2004; Hutter et al., 2000). *epi-1* (α_B-laminin), *lam-1* (β-laminin), *lam-2* (γ-laminin) and *pat-2* (α-integrin) each induced EMEs when targeted by RNAi and had significant reductions in the number of muscle arms reaching the nerve cord in either RNAi or hypomorphic mutant backgrounds (Fig. 6, Table 2). By contrast, other cell-adhesion genes that we examined by RNAi or mutations, such as all 13 predicted cadherin genes (Cox et al., 2004), conferred no EMEs (not shown). Similarly, disruption of *ina-1* (α-integrin) by RNAi or mutation did not result in EMEs (Table 2). This was a

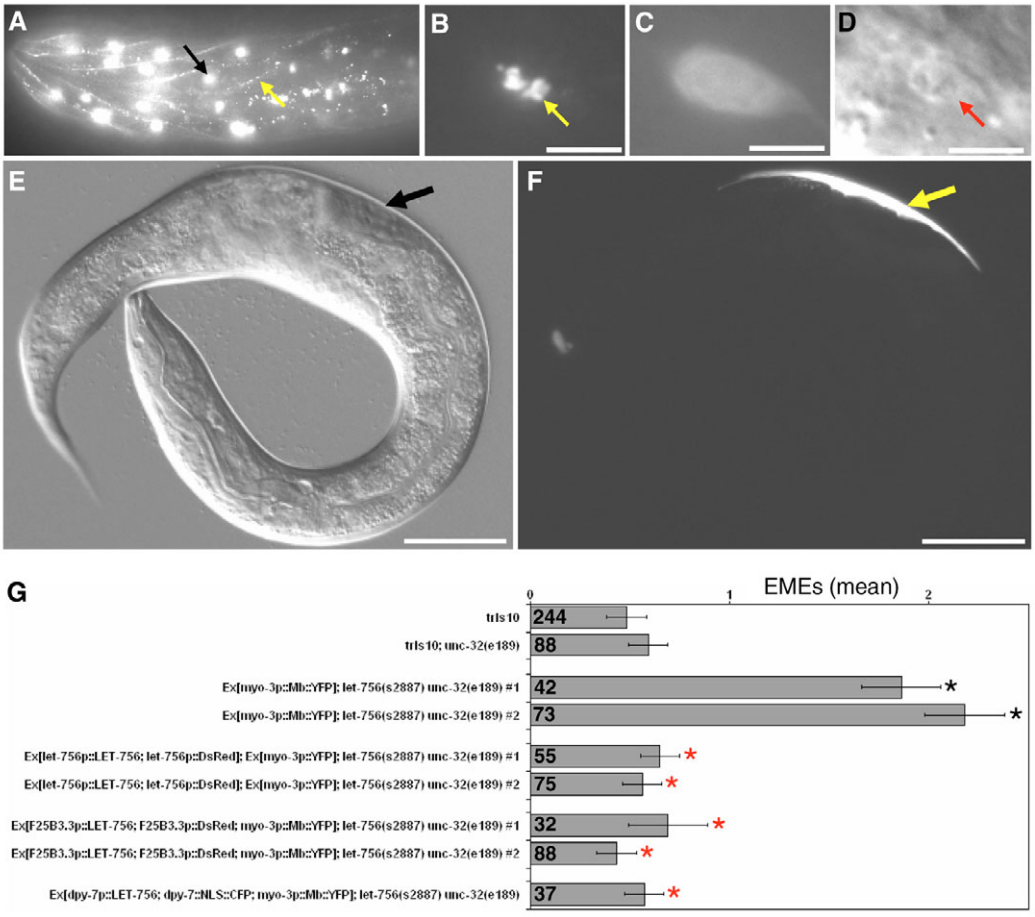

Fig. 5. *let-756* functions non-autonomously to regulate muscle membrane extension. (**A-D**) LET-756::YFP expression from RP195 *Ex[let-756p::LET-756::YFP; let-756p::DsRed]; let-756(s2887) unc-32(e189) III* animals. Scale bar: 5 μm. (A) The anterior dorsal BWMs show LET-756::YFP expression in the nucleus (black arrow) and at the sites of BWM-BWM contacts (yellow arrow). (B) Nuclear localization of LET-756::YFP (arrow) in a CAN neuron. (C) RFP channel of the same cell in B. (D) A DIC image of the same cell in B. The arrow indicates the same spot as in B. (**E**,**F**) An RP175 *Ex[let-756p::YFP; let-756p::LET-756]; let-756(s2887) unc-32(e189) III* animal. Expression of *let-756* in two BWMs (arrow, F) is sufficient to rescue the lethality associated with a *let-756(s2887)* null mutation, and can locally rescue the scrawny phenotype (arrow, E). Scale bar: 50 μm. (**G**) *let-756* expression from either the 3.0 kb *let-756* promoter/enhancer sequence, a pan-neuronal promoter (*F25B3.3p*) or a hypodermal promoter (*dpy-7p*) in a *let-756(s2887)* null background confers significantly fewer EMEs (red asterisks) than *let-756(s2887)* null escapers without the rescuing arrays ($P<0.001$). Black asterisks indicate significantly more EMEs than in *trls10* or *trls10; unc-32(e189)* controls ($P<0.001$). *n* values are indicated for each genotype within each bar and error bars represent the s.e.m.

surprising result, as the INA-1/PAT-3 integrin heterodimer probably binds laminin, while the PAT-2/PAT-3 complex probably binds UNC-52/perlecan (Baum and Garriga, 1997; Rogalski et al., 1993). However, this prompted us to examine perlecan mutants. We found that *unc-52(e998)* mutants phenocopy the MAD and EME phenotypes of *pat-2(RNAi)* (Fig. 6, Table 2). These data suggest that the PAT-2/PAT-3 integrin complex functions with laminins and perlecan to regulate muscle membrane extension.

Given the phenotypic overlap between disruptions in *pat-2*, the laminins and the FGF pathway, we asked if these components interact genetically. We tested if the *clr-1(e1745)* and *let-60(n1046)* mutants that upregulate FGF pathway activity could suppress the EMEs induced by *epi-1(RNAi)*, *lam-1(RNAi)*, *lam-2(RNAi)* and *pat-2(RNAi)*. In all cases, *clr-1(e1745)* significantly reduced the number of EMEs induced by these RNAi treatments as did *let-60(n1046)*, albeit less effectively (Fig. 6, Table 3). These results show that the FGF pathway interacts genetically with both integrin and laminins.

DISCUSSION

We have discovered that an FGF pathway is a general negative regulator of plasma membrane extension from the body wall muscles of *C. elegans*. Too little FGFR signaling results in ectopic membrane extensions and too much signaling prevents membrane extension. Using temperature-sensitive alleles of two genes in the FGF pathway, we demonstrate that FGF signaling is required during early larval development to prevent EMEs. Previous work has shown that the level of *let-756* FGF mRNA peaks during the second larval stage and declines thereafter (Roubin et al., 1999), providing additional evidence that the LET-756 FGF pathway is required during this period to inhibit EMEs. Although FGFR signaling acts in muscles to regulate membrane extension, *let-756* can be expressed from a variety of spatial locations to prevent the formation of the ectopic membrane extensions without compromising muscle arm extension. This argues against LET-756 acting as either an attractant or repellant of muscle membrane extension. Instead, we speculate that the interaction of LET-756 with EGL-15 acts as a switch to negatively regulate membrane extension by unknown molecular mechanisms.

Unlike the FGF pathway, we found that disruptions in laminin, integrin and perlecan result in both ectopic membrane extensions and fewer muscle arms reaching the nerve cord. These phenotypes are consistent with wayward muscle arm extensions that fail to reach their target. We speculate that the laminins, integrins and perlecan, which together constitute a significant part of the extracellular matrix and muscle adhesion complex (Cox and Hardin, 2004, Hutter et al., 2000), could be required to regulate the spatial distribution of factors that guide muscle arms to the nerve cord. Alternatively, disruption of laminin, integrin and perlecan may interfere with proper localization of receptors on the plasma membrane of muscles or with adhesion of the muscle membrane extensions to the substratum (Huang et al., 2003). Under any model, the ectopic membrane

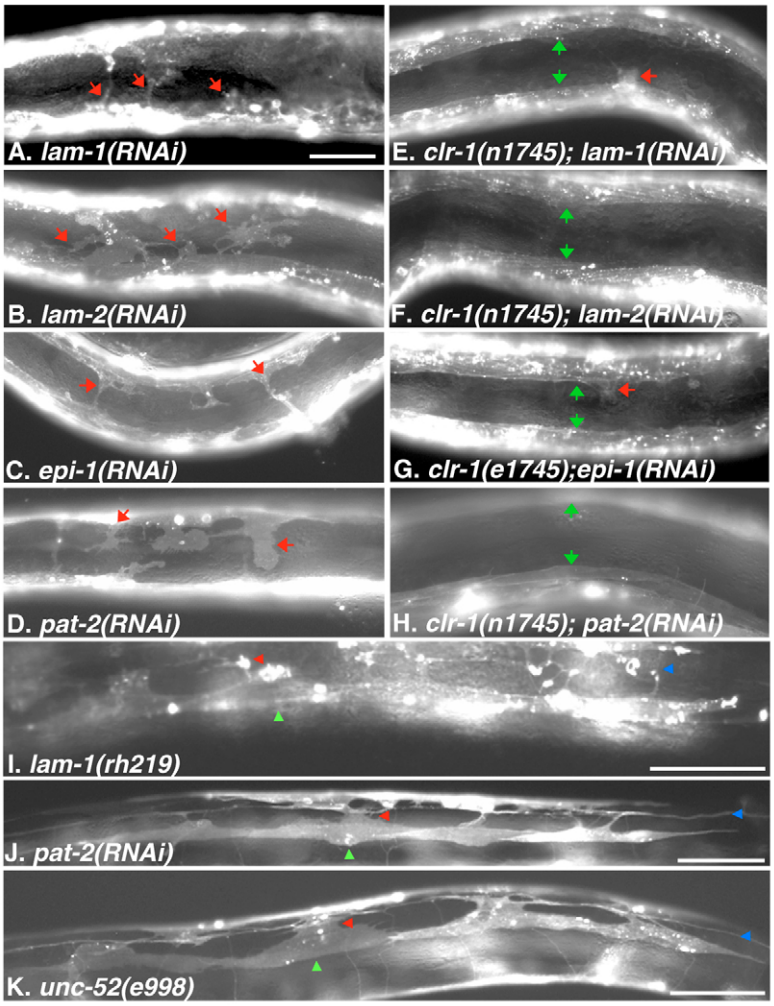

Fig. 6. Disruption of laminin and integrin genes results in EMEs that can be suppressed by *clr-1* mutants. (**A-H**) All images correspond to the boxed area in Fig. 1A. Red arrows indicate individual EMEs and green arrows indicate intact lateral BWM membranes. EMEs are seen in *trIs10* worms fed *lam-1(RNAi)* (A), *lam-2(RNAi)* (B), *epi-1(RNAi)* (C) or *pat-2(RNAi)* (D). (E-H) The EME phenotype is strongly suppressed for each genotype in the background of *clr-1(e1745)* at 20°C. (**I-K**) A dorsal right-hand side view of adult worms in the background of *trIs30*, showing BWMs numbers 9, 11, 13 (green arrowhead) and 15, right to left, according to our numbering scheme (Dixon and Roy, 2005), extending muscle arms (red arrowheads) to the dorsal nerve cord (blue arrowheads). A MAD phenotype is seen in *lam-1(rh219); trIs30* (I), *pat-2(RNAi); trIs30* (J) and *unc-52(e998); trIs30* (K) worms. Scale bar: in A, 50 μm for A-H; 50 μm in I-K.

extensions resulting from compromised laminin and integrin function depend on FGF pathway activity as increased FGFR activity suppresses their extension.

Our work demonstrates a new role for FGF signaling in *C. elegans* in which FGFR activity regulates muscle membrane extension specifically during early larval development. During this same period, EGL-15 plays at least four other roles in the animal. First, EGL-15 acts as a receptor for EGL-17, which guides the migration of the sex myoblasts to the incipient vulva (Burdine et al., 1998; Burdine et al., 1997). The *egl-15* gene encodes two isoforms by splicing between two alternative exons called 5A and 5B (Goodman et al., 2003). Null mutations that are specific to the 5A exon, including *egl-15(n484)*, reveal that only EGL-15(5A) is necessary for the guidance of the sex myoblasts and is therefore likely to be the only isoform on the sex myoblasts required to bind EGL-17 (Goodman et al., 2003). Although *egl-15(n484)* and *let-756(s2613)* mutations result in EMEs from the BWMs, the *egl-17(n1377)* null allele does not. Our observations therefore suggest that EGL-15(5A) is capable of receiving either EGL-17 or LET-756 ligands, depending on the cellular context. This conclusion is further supported by the fact that expression of LET-756 under the control of *egl-17* regulatory elements can partially rescue the sex-myoblast migration defects (Goodman et al., 2003).

The second well-established role for FGFR signaling is in fluid homeostasis. Hyperactivity of EGL-15 results in fluid filled worms, called a clear or Clr phenotype (Kokel et al., 1998). By contrast, hypomorphic *let-756* or *egl-15* alleles that do not specifically disrupt EGL-15A result in a scrawny phenotype that is consistent with the worms lacking sufficient fluid (DeVore et al., 1995; Roubin et al., 1999). The null phenotype of *let-756* or *egl-15* is early larval lethality, which probably results from improper fluid regulation (Birnbaum et al., 2005; Huang and Stern, 2005). Recent work has demonstrated that EGL-15 activity in the hypodermis is essential for fluid regulation and that LET-756 probably signals to EGL-15 in the hypodermis from the BWMs (Huang and Stern, 2004). These results are seemingly contradictory to our observations that LET-756 expression from a transgenic array can rescue the essential *let-756* function from any number of cells, including a single BWM, a single CAN neuron or a limited number of cells in the pharynx. However, this difference can be reconciled by noting that the specific requirement of LET-756 in BWMs was determined by Huang and Stern (Huang and Stern, 2004) using a free chromosomal duplication, while we used a transgenic array that typically results in transgene overexpression (Mello et al., 1991). We therefore suggest that overexpression of LET-756 from few cells of any type might be sufficient to regulate fluid balance and that the ligand can travel some distance within the animal to trigger EGL-15 activity.

A third role for EGL-15 is in axon extension, guidance and the positional maintenance of two interneuron axons along the ventral midline (Bulow et al., 2004). We believe that EMEs are not a secondary consequence of compromising these roles of EGL-15 for many reasons. First, the *egl-15(n484)* allele has no axonal guidance

Table 3. Disruption of cell adhesion or the extracellular matrix results in EMEs

	Genotype*	Description	*n*	EMEs†	*P* value‡	*P* value‡
A screen of 847 Unc and Prz genes identifies components of the integrin complex and the ECM						
1	*Ø(RNAi)*	Wild type	157	0.6±0.7	–	–
2	*pat-4(RNAi)*	Integrin-linked kinase	36	2.9±1.9	<0.001 (1)	–
3	*pat-6(RNAi)*	Actopaxin	43	3.0±2.0	<0.001 (1)	–
4	*lam-1(RNAi)*	β-Laminin	40	4.1±1.7	<0.001 (1)	–
5	*lam-2(RNAi)*	γ-Laminin	38	4.4±2.8	<0.001 (1)	–
6	*epi-1(RNAi)*	αB-laminin	86	3.2±1.7	<0.001 (1)	–
7	*pat-2(RNAi)*	α-Integrin	88	3.5±2.5	<0.001 (1)	–
8	*ina-1(RNAi)*	α-Integrin	88	0.5±0.7	>0.05 (1)	–
9	*unc-52(RNAi)*	Perlecan	44	1.8±1.2	<0.001 (1)	–
10	*lam-1(rh219)*	β-Laminin (hypomorph)	40	1.7±1.6	<0.001 (1)	–
11	*epi-1(rh152)*	αB-laminin (hypomorph)	44	3.0±2.4	<0.001 (1)	–
12	*ina-1(gm144)*	α-Integrin (hypomorph)	44	0.6±0.9	>0.05 (1)	–
***clr-1* loss of function and *let-60* gain of function suppresses the EME phenotype of *pat-2* and the laminin complex**						
13	*clr-1(e1745)* 20°C	RPTP (hypomorph)	21	0.6±2.5	–	–
15	*clr-1(e1745); lam-1(RNAi)*		58	1.0±1.1	<0.001 (4)	<0.001 (13)
14	*clr-1(e1745); lam-2(RNAi)*		60	1.0±1.2	<0.001 (5)	<0.001 (13)
16	*clr-1(e1745); epi-1(RNAi)*		48	0.7±0.8	<0.001 (6)	>0.05 (13)
17	*clr-1(e1745); pat-2(RNAi)*		61	0.7±1.0	<0.001 (7)	>0.05 (13)
18	*let-60(n1046)*	Ras GTPase (gain of function)	44	0.8±0.8	–	–
19	*let-60(n1046); lam-1(RNAi)*		27	3.1±1.0	<0.001 (4)	<0.001 (18)
20	*let-60(n1046); lam-2(RNAi)*		25	3.0±1.6	<0.001 (5)	<0.001 (18)
21	*let-60(n1046); epi-1(RNAi)*		60	2.6±1.6	<0.001 (6)	<0.001 (18)
22	*let-60(n1046); pat-2(RNAi)*		71	2.3±2.2	<0.001 (7)	<0.001 (18)

*The *trls10* background was used for all counts. Unless otherwise indicated, all counts used late L4 or young adult worms from mixed-stage populations maintained at 20°C.
†All EME counts represent the mean±s.d.
‡*P* values derived from Student's *t*-test with respect to the appropriate negative control (comparison row indicated in brackets).

defects (Bulow et al., 2004), but does result in severe EMEs. Second, the cellular focus of EGL-15 in axon extension and guidance is in the hypodermis (Bulow et al., 2004), whereas we have demonstrated that *egl-15* and *sem-5* are both autonomously required within the BWMs to antagonize EMEs. Third, EGL-15 is required embryonically for axon extension and guidance (Bulow et al., 2004), whereas our temperature-shift time-course experiments using temperature-sensitive alleles demonstrated that *egl-15* and *sos-1* are dispensable during embryonic development to prevent EMEs. Fourth, the motor axon extension and guidance defects of *egl-15* nulls are relatively minor, being restricted to a single anterior commissure (Bulow et al., 2004), whereas we observe EMEs all along the entire length of the animal. Fifth, the role of EGL-15 in the maintenance of axon position is restricted to two ventral cord interneurons and does not require the intracellular domains of EGL-15 (Bulow et al., 2004). These observations are inconsistent with EMEs being induced by defects in the maintenance of axon position because the *egl-15(n1783)* mutation that specifically disrupts the EGL-15 kinase domain (Goodman et al., 2003) results in EMEs, along with other intracellular transducers of the EGL-15 signal, including *sem-5*, *sos-1* and *let-60*. Last, we did not observe EMEs projecting to any particular axon in the lateral hypodermal ridge in FGFR mutants. We therefore conclude that the aberrant membrane projections that result from compromised FGFR signaling are not a secondary consequence of defects in axon extension, guidance or positional maintenance.

Finally, an FGF pathway is required for acetylcholine receptor (AChR) expression at the neuromuscular junction in *C. elegans* (Gottschalk et al., 2005). *egl-15* acts in parallel with *cam-1*, which encodes a ROR-family receptor tyrosine kinase ortholog, to regulate the presence of AChRs at the NMJ, without altering the transcription levels of AChR subunits (Gottschalk et al., 2005). We have examined several mutants involved in neurotransmission at the neuromuscular junction, including *cam-1*/ROR (Francis et al., 2005), *unc-18*/UNC-18 (Weimer et al., 2003), *cha-1*/choline acetyltransferase (Alfonso et al., 1994), *unc-29*/nicotinic AChR subunit (Fleming et al., 1997) and *unc-25*/glutamic acid decarboxylase (Jin et al., 1999), none of which have muscle membrane extension defects (S.J.D. and P.J.R., unpublished). This suggests that neurotransmission does not regulate muscle membrane extension. However, the work of Gottschalk and colleagues raises the exciting possibility that the FGF pathway may regulate the localization or membrane insertion of other receptors that regulate BWM membrane extension.

We gratefully acknowledge Andrew Spence for many helpful comments and use of his equipment, Michael Stern for strains and helpful comments, Oliver Hobert for strains and the *egl-15(5A)* cDNA, Craig Hunter for the *sid-1(qt9)* null mutant, and Zhibin Lu and Jason Moffat for the construction of several transgenes. We also thank Theresa Stiernagle and the *C. elegans* Genetic Center, which is funded by the NIH National Center for Research Resources (NCRR), for sending us many worm strains. S.J.D. is supported by a pre-doctoral scholarship from the Natural Sciences and Engineering Research Council of Canada. P.J.R. is a Canadian Research Chair in Molecular Neurobiology. This work was supported by a National Cancer Institute of Canada operating grant, a Terry Fox equipment grant, and infrastructure awards from the Canadian Foundation for Innovation and Ontario Innovation Trust.

Supplementary material

Supplementary material for this article is available at
http://dev.biologists.org/cgi/content/full/133/7/1263/DC1

References

Alfonso, A., Grundahl, K., McManus, J. R. and Rand, J. B. (1994). Cloning and characterization of the choline acetyltransferase structural gene (cha-1) from C. elegans. *J. Neurosci.* **14**, 2290-2300.
Bate, M. (1990). The embryonic development of larval muscles in Drosophila. *Development* **110**, 791-804.
Baum, P. D. and Garriga, G. (1997). Neuronal migrations and axon fasciculation are disrupted in ina-1 integrin mutants. *Neuron* **19**, 51-62.

Birnbaum, D., Popovici, C. and Roubin, R. (2005). A pair as a minimum: the two fibroblast growth factors of the nematode Caenorhabditis elegans. *Dev. Dyn.* **232**, 247-255.
Borland, C. Z., Schutzman, J. L. and Stern, M. J. (2001). Fibroblast growth factor signaling in Caenorhabditis elegans. *BioEssays* **23**, 1120-1130.
Bulow, H. E., Boulin, T. and Hobert, O. (2004). Differential functions of the C. elegans FGF receptor in axon outgrowth and maintenance of axon position. *Neuron* **42**, 367-374.
Burdine, R. D., Chen, E. B., Kwok, S. F. and Stern, M. J. (1997). egl-17 encodes an invertebrate fibroblast growth factor family member required specifically for sex myoblast migration in Caenorhabditis elegans. *Proc. Natl. Acad. Sci. USA* **94**, 2433-2437.
Burdine, R. D., Branda, C. S. and Stern, M. J. (1998). EGL-17(FGF) expression coordinates the attraction of the migrating sex myoblasts with vulval induction in C. elegans. *Development* **125**, 1083-1093.
Clark, S. G., Stern, M. J. and Horvitz, H. R. (1992). C. elegans cell-signalling gene sem-5 encodes a protein with SH2 and SH3 domains. *Nature* **356**, 340-344.
Cox, E. A. and Hardin, J. (2004). Sticky worms: adhesion complexes in C. elegans. *J. Cell Sci.* **117**, 1885-1897.
Cox, E. A., Tuskey, C. and Hardin, J. (2004). Cell adhesion receptors in C. elegans. *J. Cell Sci.* **117**, 1867-1870.
DeChiara, T. M., Bowen, D. C., Valenzuela, D. M., Simmons, M. V., Poueymirou, W. T., Thomas, S., Kinetz, E., Compton, D. L., Rojas, E., Park, J. S. et al. (1996). The receptor tyrosine kinase MuSK is required for neuromuscular junction formation in vivo. *Cell* **85**, 501-512.
DeVore, D. L., Horvitz, H. R. and Stern, M. J. (1995). An FGF receptor signaling pathway is required for the normal cell migrations of the sex myoblasts in C. elegans hermaphrodites. *Cell* **83**, 611-620.
Dickson, B. J. (2002). Molecular mechanisms of axon guidance. *Science* **298**, 1959-1964.
Dixon, S. J. and Roy, P. J. (2005). Muscle arm development in Caenorhabditis elegans. *Development* **132**, 3079-3092.
Feinberg, E. H. and Hunter, C. P. (2003). Transport of dsRNA into cells by the transmembrane protein SID-1. *Science* **301**, 1545-1547.
Fire, A., Xu, S., Montgomery, M. K., Kostas, S. A., Driver, S. E. and Mello, C. C. (1998). Potent and specific genetic interference by double-stranded RNA in Caenorhabditis elegans. *Nature* **391**, 806-811.
Fleming, J. T., Squire, M. D., Barnes, T. M., Tornoe, C., Matsuda, K., Ahnn, J., Fire, A., Sulston, J. E., Barnard, E. A., Sattelle, D. B. et al. (1997). Caenorhabditis elegans levamisole resistance genes lev-1, unc-29, and unc-38 encode functional nicotinic acetylcholine receptor subunits. *J. Neurosci.* **17**, 5843-5857.
Folkman, J. (1971). Tumor angiogenesis: therapeutic implications. *N. Engl. J. Med.* **285**, 1182-1186.
Francis, M. M., Evans, S. P., Jensen, M., Madsen, D. M., Mancuso, J., Norman, K. R. and Maricq, A. V. (2005). The Ror receptor tyrosine kinase CAM-1 is required for ACR-16-mediated synaptic transmission at the C. elegans neuromuscular junction. *Neuron* **46**, 581-594.
Gautam, M., Noakes, P. G., Moscoso, L., Rupp, F., Scheller, R. H., Merlie, J. P. and Sanes, J. R. (1996). Defective neuromuscular synaptogenesis in agrin-deficient mutant mice. *Cell* **85**, 525-535.
Goodman, S. J., Branda, C. S., Robinson, M. K., Burdine, R. D. and Stern, M. J. (2003). Alternative splicing affecting a novel domain in the C. elegans EGL-15 FGF receptor confers functional specificity. *Development* **130**, 3757-3766.
Gottschalk, A., Almedom, R. B., Schedletzky, T., Anderson, S. D., Yates, J. R., 3rd and Schafer, W. R. (2005). Identification and characterization of novel nicotinic receptor-associated proteins in Caenorhabditis elegans. *EMBO J.* **24**, 2566-2578.
Hall, D. H. and Hedgecock, E. M. (1991). Kinesin-related gene unc-104 is required for axonal transport of synaptic vesicles in C. elegans. *Cell* **65**, 837-847.
Hedgecock, E. M., Culotti, J. G. and Hall, D. H. (1990). The unc-5, unc-6, and unc-40 genes guide circumferential migrations of pioneer axons and mesodermal cells on the epidermis in C. elegans. *Neuron* **4**, 61-85.
Huang, C. C., Hall, D. H., Hedgecock, E. M., Kao, G., Karantza, V., Vogel, B. E., Hutter, H., Chisholm, A. D., Yurchenco, P. D. and Wadsworth, W. G. (2003). Laminin alpha subunits and their role in C. elegans development. *Development* **130**, 3343-3358.
Huang, P. and Stern, M. J. (2004). FGF signaling functions in the hypodermis to regulate fluid balance in C. elegans. *Development* **131**, 2595-2604.
Huang, P. and Stern, M. J. (2005). FGF signaling in flies and worms: more and more relevant to vertebrate biology. *Cytokine Growth Factor Rev.* **16**, 151-158.
Hutter, H., Vogel, B. E., Plenefisch, J. D., Norris, C. R., Proenca, R. B., Spieth, J., Guo, C., Mastwal, S., Zhu, X., Scheel, J. et al. (2000). Conservation and novelty in the evolution of cell adhesion and extracellular matrix genes. *Science* **287**, 989-994.
Jin, Y., Jorgensen, E., Hartwieg, E. and Horvitz, H. R. (1999). The Caenorhabditis elegans gene unc-25 encodes glutamic acid decarboxylase and is required for synaptic transmission but not synaptic development. *J. Neurosci.* **19**, 539-548.
Kamath, R. S. and Ahringer, J. (2003). Genome-wide RNAi screening in Caenorhabditis elegans. *Methods* **30**, 313-321.
Kamath, R. S., Fraser, A. G., Dong, Y., Poulin, G., Durbin, R., Gotta, M., Kanapin, A., Le Bot, N., Moreno, S., Sohrmann, M. et al. (2003). Systematic functional analysis of the Caenorhabditis elegans genome using RNAi. *Nature* **421**, 231-237.
Keilhack, H., Muller, M., Bohmer, S. A., Frank, C., Weidner, K. M., Birchmeier, W., Ligensa, T., Berndt, A., Kosmehl, H., Gunther, B. et al. (2001). Negative regulation of Ros receptor tyrosine kinase signaling. An epithelial function of the SH2 domain protein tyrosine phosphatase SHP-1. *J. Cell Biol.* **152**, 325-334.
Kokel, M., Borland, C. Z., DeLong, L., Horvitz, H. R. and Stern, M. J. (1998). clr-1 encodes a receptor tyrosine phosphatase that negatively regulates an FGF receptor signaling pathway in Caenorhabditis elegans. *Genes Dev.* **12**, 1425-1437.
Kullberg, R. W., Lentz, T. L. and Cohen, M. W. (1977). Development of the myotomal neuromuscular junction in Xenopus laevis: an electrophysiological and fine-structural study. *Dev. Biol.* **60**, 101-129.
Lewis, J. A. and Fleming, J. T. (1995). Basic culture methods. *Methods Cell Biol.* **48**, 3-29.
Lin, X., Qadota, H., Moerman, D. G. and Williams, B. D. (2003). C. elegans PAT-6/actopaxin plays a critical role in the assembly of integrin adhesion complexes in vivo. *Curr. Biol.* **13**, 922-932.
Lowenstein, E. J., Daly, R. J., Batzer, A. G., Li, W., Margolis, B., Lammers, R., Ullrich, A., Skolnik, E. Y., Bar-Sagi, D. and Schlessinger, J. (1992). The SH2 and SH3 domain-containing protein GRB2 links receptor tyrosine kinases to ras signaling. *Cell* **70**, 431-442.
Lundquist, E. A., Herman, R. K., Shaw, J. E. and Bargmann, C. I. (1998). UNC-115, a conserved protein with predicted LIM and actin-binding domains, mediates axon guidance in C. elegans. *Neuron* **21**, 385-392.
Mackinnon, A. C., Qadota, H., Norman, K. R., Moerman, D. G. and Williams, B. D. (2002). C. elegans PAT-4/ILK functions as an adaptor protein within integrin adhesion complexes. *Curr. Biol.* **12**, 787-797.
Mello, C. C., Kramer, J. M., Stinchcomb, D. and Ambros, V. (1991). Efficient gene transfer in C. elegans: extrachromosomal maintenance and integration of transforming sequences. *EMBO J.* **10**, 3959-3970.
Misgeld, T., Burgess, R. W., Lewis, R. M., Cunningham, J. M., Lichtman, J. W. and Sanes, J. R. (2002). Roles of neurotransmitter in synapse formation: development of neuromuscular junctions lacking choline acetyltransferase. *Neuron* **36**, 635-648.
Moghal, N. and Sternberg, P. W. (2003). The epidermal growth factor system in Caenorhabditis elegans. *Exp. Cell Res.* **284**, 150-159.
Ogawa, K., Pasqualini, R., Lindberg, R. A., Kain, R., Freeman, A. L. and Pasquale, E. B. (2000). The ephrin-A1 ligand and its receptor, EphA2, are expressed during tumor neovascularization. *Oncogene* **19**, 6043-6052.
Okkema, P. G., Harrison, S. W., Plunger, V., Aryana, A. and Fire, A. (1993). Sequence requirements for myosin gene expression and regulation in Caenorhabditis elegans. *Genetics* **135**, 385-404.
Plate, K. H., Breier, G., Weich, H. A. and Risau, W. (1992). Vascular endothelial growth factor is a potential tumour angiogenesis factor in human gliomas in vivo. *Nature* **359**, 845-848.
Pollard, T. D. and Borisy, G. G. (2003). Cellular motility driven by assembly and disassembly of actin filaments. *Cell* **112**, 453-465.
Popovici, C., Conchonaud, F., Birnbaum, D. and Roubin, R. (2004). Functional phylogeny relates LET-756 to fibroblast growth factor 9. *J. Biol. Chem.* **279**, 40146-40152.
Ritzenthaler, S., Suzuki, E. and Chiba, A. (2000). Postsynaptic filopodia in muscle cells interact with innervating motoneuron axons. *Nat. Neurosci.* **3**, 1012-1017.
Rocheleau, C. E., Howard, R. M., Goldman, A. P., Volk, M. L., Girard, L. J. and Sundaram, M. V. (2002). A lin-45 raf enhancer screen identifies eor-1, eor-2 and unusual alleles of Ras pathway genes in Caenorhabditis elegans. *Genetics* **161**, 121-131.
Rogalski, T. M., Williams, B. D., Mullen, G. P. and Moerman, D. G. (1993). Products of the unc-52 gene in Caenorhabditis elegans are homologous to the core protein of the mammalian basement membrane heparan sulfate proteoglycan. *Genes Dev.* **7**, 1471-1484.
Rorth, P. (2003). Communication by touch: role of cellular extensions in complex animals. *Cell* **112**, 595-598.
Roubin, R., Naert, K., Popovici, C., Vatcher, G., Coulier, F., Thierry-Mieg, J., Pontarotti, P., Birnbaum, D., Baillie, D. and Thierry-Mieg, D. (1999). let-756, a C. elegans fgf essential for worm development. *Oncogene* **18**, 6741-6747.
Simmer, F., Moorman, C., van der Linden, A. M., Kuijk, E., van den Berghe, P. V., Kamath, R., Fraser, A. G., Ahringer, J. and Plasterk, R. H. (2003). Genome-wide RNAi of C. elegans using the hypersensitive rrf-3 strain reveals novel gene functions. *PLoS Biol.* **1**, E12.
Stern, M. J., Marengere, L. E., Daly, R. J., Lowenstein, E. J., Kokel, M., Batzer, A., Olivier, P., Pawson, T. and Schlessinger, J. (1993). The human GRB2 and Drosophila Drk genes can functionally replace the Caenorhabditis elegans cell signaling gene sem-5. *Mol. Biol. Cell* **4**, 1175-1188.

Stretton, A. O. (1976). Anatomy and development of the somatic musculature of the nematode Ascaris. *J. Exp. Biol.* **64**, 773-788.
Sulston, J. E. and Horvitz, H. R. (1977). Post-embryonic cell lineages of the nematode, Caenorhabditis elegans. *Dev. Biol.* **56**, 110-156.
Sulston, J. E., Schierenberg, E., White, J. G. and Thomson, J. N. (1983). The embryonic cell lineage of the nematode Caenorhabditis elegans. *Dev. Biol.* **100**, 64-119.
Sundaram, M., Yochem, J. and Han, M. (1996). A Ras-mediated signal transduction pathway is involved in the control of sex myoblast migration in Caenorhabditis elegans. *Development* **122**, 2823-2833.
Timmons, L. and Fire, A. (1998). Specific interference by ingested dsRNA. *Nature* **395**, 854.
Timmons, L., Court, D. L. and Fire, A. (2001). Ingestion of bacterially expressed dsRNAs can produce specific and potent genetic interference in Caenorhabditis elegans. *Gene* **263**, 103-112.
Uhm, C. S., Neuhuber, B., Lowe, B., Crocker, V. and Daniels, M. P. (2001). Synapse-forming axons and recombinant agrin induce microprocess formation on myotubes. *J. Neurosci.* **21**, 9678-9689.
Weimer, R. M., Richmond, J. E., Davis, W. S., Hadwiger, G., Nonet, M. L. and Jorgensen, E. M. (2003). Defects in synaptic vesicle docking in unc-18 mutants. *Nat. Neurosci.* **6**, 1023-1030.
White, J. G., Southgate, E., Thomson, J. N. and Brenner, S. (1976). The structure of the ventral nerve cord of Caenorhabditis elegans. *Philos. Trans. R. Soc. Lond. B Biol. Sci.* **275**, 327-348.
White, J. G., Southgate, E., Thomson, J. N. and Brenner, S. (1986). The structure of the nervous system of the nematode C. elegans. *Philos. Trans. R. Soc. Lond. B Biol. Sci.* **314**, 1-340.
Winston, W. M., Molodowitch, C. and Hunter, C. P. (2002). Systemic RNAi in C. elegans requires the putative transmembrane protein SID-1. *Science* **295**, 2456-2459.